Asian Journal of Chemistry; Vol. 35, No. 2 (2023), 327-336

ASIAN JOURNAL OF CHEMISTRY

https://doi.org/10.14233/ajchem.2023.24036

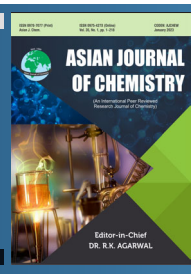

Novel Gold(III), Palladium(II) and Copper(II) Schiff Base Complexes Derived from 1-Hydroxy-2-acetonaphthone and Phenylethyl Amine: Synthesis, Characterization and Biological Studies

D.V. BONDAR and V.S. INGLE*

Department of Chemistry, Shri Chhatrapati Shivaji College, Omerga-413606, India

*Corresponding author: E-mail: inglevilas71@gmail.com

Received: 9 September 2022; *Accepted*: 31 October 2022; *Published online*: 30 January 2023; AJC-21113

In this work, a novel Schiff base from 1-hydroxy-2-acetonaphthone and phenyl ethylamine and its metal complexes were synthesized and characterized using UV-visible, FT-IR, ^{1}H and ^{13}C NMR, SC-XRD, LCMS, TGA-DSC and powder X-ray diffraction. The IR data indicated that the ligand was coordinated *via* bidentate bonding through the oxygen atom of naphthone and nitrogen atom of azomethine unit. The TGA-DSC analysis of Au(III), Pd(II), and Cu(II) revealed the presence of coordinated water molecules. According to powder X-ray diffraction data, the Schiff base ligand exhibits a tetragonal crystal structure, Au(III) complex has a cubic crystal structure, while Pd(II) and Cu(II) complexes have monoclinic crystal structures. The synthesized metal complexes were examined for their *in vitro* antibacterial bioactivity against the Gram-negative bacteria *E. coli, P. aeruginosa* and Gram-positive *S. aureus, B. subtilis* as well as their *in vitro* antifungal activity against the two fungus *C. albicans* and *A. niger*. According to the biological findings, the synthesized metal complexes exhibited better antimicrobial activities compared to the Schiff base ligand. Similar, outcomes were followed in the antioxidant activity analysis, where the synthesized Schiff base metal complexes had DPPH radical scavenging activity.

Keywords: Schiff base, 1-Hydroxy-2-acetonaphthone, Phenylethyl amine, Metal Complexes.

INTRODUCTION

The exploration of novel Schiff base ligands has been related to the several recent important breakthrough in the coordination chemistry [1,2]. Schiff base ligands are also known as azomethines, imines or anils and regarded as most versatile ligands, since they are typically formed through simple condensation between aldehydes, ketones and primary amines [3]. Scientists in the medical profession have taken an interest in Schiff base and its transition metal complexes due to their distinct ligation behaviour, significant physico-chemical features and potentially used as new therapeutic agents [4,5], moreover it exhibits anti-COVID action too [6,7].

Naphthalene based compounds play an important role in vast range of pathophysiological conditions, such as antimicrobial, antineurodegenerative, antidepressant, anti-inflammatory, anticancer, antiviral activities [8]. Consequently, a crucial building component in the realm of drug development, naphthalene scaffolds exhibit a wide range of biological actions according to their various structural alterations [9]. All these pharmacological applications are very much influenced by the structural arrangement of the compounds, particularly the coordination number and substituted atoms of the Schiff bases, which can tuned the templating effect of the metal ion [10].

1-Hydroxy-2-acetonaphthone (HAN), a two-ring analog of methyl salicylate, is used for formation of spiro naphthoxazine dimers [11], chromone compounds [12], *etc*. Furthermore, it is thought to catalyze several organic reactions [13], facilitate intramolecular proton transfer (ESIPT) for fluorescence environment [14] and function as a chemosensor for the selective detection of hazardous ions [15]. Several HAN Schiff base metal complexes are also extensively reported as antioxidant [16], antimicrobial [17], anticancer [18,19], anti-inflammatory [20], antiviral [21], anti-HIV [22] activities.

To best of our knowledge till date, no published literature on the condensation of 1-hydroxy-2-acetonaphthone (HAN) and phenylethylamine (PEA) which is to produce a Schiff base 2-(1-(phenethylimino)ethyl)naphthalen-1-ol is reported yet.

Therefore, the present research was focused on the synthesis of new Schiff base and its metal complexes with Au(III), Pd(II) and Cu(II) and characterized through physico-chemical properties, various spectroscopic techniques and also evaluated their antibacterial, antifungal, antioxidant bioactivities, as well as computational structural investigations.

EXPERIMENTAL

The AR grade chemicals and solvents, including 1-hydroxy-2-aceto-naphthone, phenylethylamine, metal chlorides and acetates, ethyl acetate, *n*-hexane, HPLC grade methanol and absolute ethanol were procured from Sigma-Aldrich and used as such. *In vitro* antibacterial activity was screened by using Mueller-Hinton Agar (MHA) obtained from Hi-media, Mumbai, India. In laboratory, TLC Alu foil silica gel 60 F_{254} was used to monitor the reaction's progress. Compounds melting points were conducted in an open capillary and recorded on the using the digital instrument Kofler Bench and are uncorrected.

Characterization: For elemental analysis, a Perkin-Elmer 240 elemental analyzer was employed. The UV-Vis spectra of the compounds were obtained using a Shimadzu UV-1800 240V spectrophotometer and methanol as solvent in the range 200-600 nm. The FT-IR spectra in the range 4000-650 cm^{-1} were recorded using KBr discs on a Bruker Alpha II instrument. Bruker AVANCE NEO 400 MHz spectrometer with $CDCl_3$ solvent and tetramethyl silane (TMS) as an internal reference standard was used to record ^1H and ^{13}C NMR spectra. The LCMS mass spectra were recorded using a single quadrupole Agilent 1290 G7104A, model LCMSD G6125B MSD, having a scan range of 100 *m/z* to 1400 *m/z*. A single crystal analysis of the ligand detected on the Bruker D8 VENTURE by the radiation type Mo*K*α at wavelength 0.71073 Å using a voltage of 50.0 amp. The Powder XRD spectra of the synthesized Schiff base ligand and its metal complexes were recorded using a Desktop X-ray Diffractometer MiniFlex II with a range of 10-80º at the wavelength of 1.540598 Å. TGA-DSC analysis of complexes ware performed on the SDT Q600 instrument using an alumina crucible in a nitrogen gas environment with a flow rate of 100 mL/min and a heating rate of 10 ºC/min.

Antibacterial activity: Gram-negative bacteria *Escherichia coli*, *Pseudomonas aeruginosa* and Gram-positive *Staphylococcus aureus*, *Bacillus subtilis* have been used for examine the antibacterial activity of newly synthesized compounds. The Mueller Hinton Agar (MHA) plates were spread and inoculated with 100 µL of log cultures of all the microorganisms (adjusted to 0.5 McFarland Unit) and followed by placing the discs containing 10 µL of different concentration (0 to 1000 mg/mL). One disc in each plate was loaded with DMSO solvent alone which served as vehicle control and ciprofloxacin (2 mg/mL, 20 µg) was taken as positive control. The plates of test organism were incubated at 37 ºC for 24 h and clear zones obtained around the disc were measured and recorded.

Antifungal activity: The antifungal activity of the synthesized Schiff base and its three metal complexes was investigated using two fungi *viz*. *Candida albicans* and *Aspergillus niger*. The Mueller-Hinton Agar (MHA) and Potato Dextrose Agar (PDA) plates were spread and inoculated with 100 µL of cultures of both fungal strains, *C. albicans* and *A. niger*, respectively (adjusted to 0.5 McFarland unit) and followed by placing the discs containing 10 µL of different concentration (0 to 1000 µg/mL). One disc in each plate was loaded with DMSO solvent alone, which served as vehicle control. The plates of *C. albicans* were incubated at 37 ºC for 24 h and *A. niger* were incubated at 32 ºC for 24 to 74 h. The obtained zone around the disc were measured and recorded.

Antioxidant activity: Different stock (5 µL) of the test compound (0-2500 µg/mL) was added to 0.1 mL of 0.1 mM DPPH solution in a 96-well plate. The reaction set was prepared containing 0.2 mL DMSO/methanol and 5 µL of different concentrations (0-2500 µg/mL). The plate was incubated for 30 min in dark. At the end of the incubation, the decolorization was measured at 495 nm using a microplate reader (iMark, BioRad). For the antioxidant activity, ascorbic acid was served as standard. Reaction mixture containing 20 µL of deionized water was served as control. With reference to a control compound's absorbance, the percentage of DPPH free radicals that each concentration of test compounds scavenged was computed using the following equation:

$$\text{DPPH scavenging activity} = \frac{A_{control} - A_{sample}}{A_{control}} \times 100$$

Synthesis of ligand (HL): Following the reported procedure [23], 1-hydroxy-2-acetonaphthone (HAN) (0.186 g, 1 mmol) and phenylethylamine (PEA) (0.120 g, 1 mmol) in absolute ethanol (20 mL) was refluxed in a 1:1 molar ratio in the presence of catalytic quantity of glacial acetic acid (2-3 drops) for around 3 h. Reaction mixture was kept overnight for obtaining the best results (**Scheme-I**). Fine needle shaped lemon-yellow coloured crystals (HL) was filtered off, washed with hot water and recrystallized by the use of absolute ethanol, the crystals of HL ligand were obtained by slowly evaporating methanol solvent.

(*E*)-2-(1-(Phenethylimino)ethyl)naphthalen-1-ol (HL): m.f.: $C_{20}H_{19}NO$, *m.w.*: 289.38, yield: 271.46 mg (87%), colour:

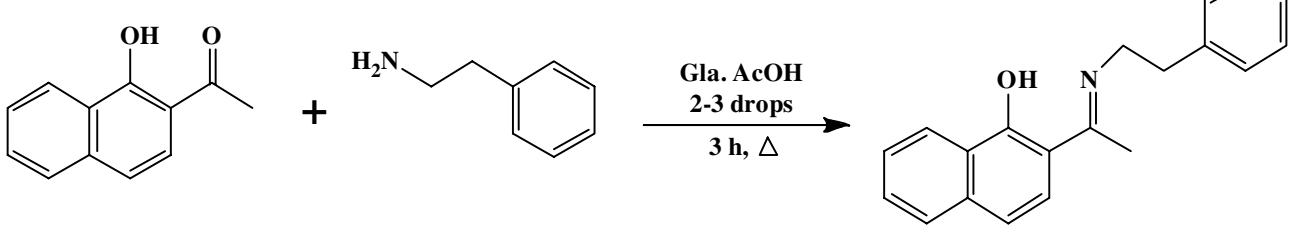

Scheme-I: Proposed synthesis of Schiff base ligand (HL)

lemon-yellow, m.p.: 122-124 ºC. Elemental analysis calcd. (found) %: C, 82.97 (83.01); H, 6.59 (6.62); N, 4.81 (4.84); O, 5.49 (5.53). FT-IR (KBr, ν_{max}, cm^{-1}): 3424.01 (OH), 1591.53 (C=N), 1526.46-1452.91 (C=C), 1271.38 (C-O), 1022.21 (C-N-C). ^{1}H NMR (400 $CDCl_3$), δ (ppm): 2.255 (s, -CH_3, 3H), 3.107 (t, -CH_2-, 2H), 3.820 (t, N-CH_2, 2H), 6.774-8.539 (m, Ar-H, 11H), 16.414 (s, Ar-OH, 1H). ^{13}C NMR ($CDCl_3$), δ (ppm): 13.585 (N=C-$\underline{C}H_3$), 36.42 (-CH_2-$\underline{C}$-Ar), 46.327 (-N-$\underline{C}H_2$-), 108.086-137.718 (Ar-$\underline{C}$), 170.768 (Ar-$\underline{C}$-OH), 175.789 (-$\underline{C}$=N-). ESI-MS (*m/z*): 290.2.

Synthesis of metal complexes [M(L)$_2$]: Following the reported procedure [24], methanol was used as solvent when added to $HAuCl_4 \cdot 3H_2O$ (0.393 g), $Pd(OAc)_2$ (0.224 g) and $Cu(OAc)_2 \cdot H_2O$ (0.199 g) (1 mmol) in the Schiff base ligand (HL) (0.578 g, 2 mmol) solution. The pH of reaction mixture was maintained around 7-8 by adding triethylamine. The resulting solution was refluxed with continuous stirring for 5 h. Before filtering, the coloured solid material was allowed to cool at ambient temperature (**Scheme-II**). The solid was filtered off and thoroughly washed with dry diethyl ether followed by minimum amount of methanol.

Au^{III}(L)$_2$ complex [*bis*((2-((*E*)-1-(phenethylimino)ethyl)-naphthalen-1-yl)oxy)gold]: m.f.: $C_{40}H_{36}N_2O_2Au$, *m.w.*: 773.71, yield: 420.14 mg (43%), colour: golden, m.p.: < 300 ºC. Elemental analysis calcd. (found) %: C, 62.05 (62.10); H, 4.61 (4.69); N, 3.53 (3.62); O, 4.08 (4.14); Au, 25.42 (25.46). FT-IR (KBr, ν_{max}, cm^{-1}): 1577.70 (C=N), 1557.07-1434.03 (C=C), 1256.50 (C-O), 1021.58 (C-N-C). ^{1}H NMR (400, $CDCl_3$), δ

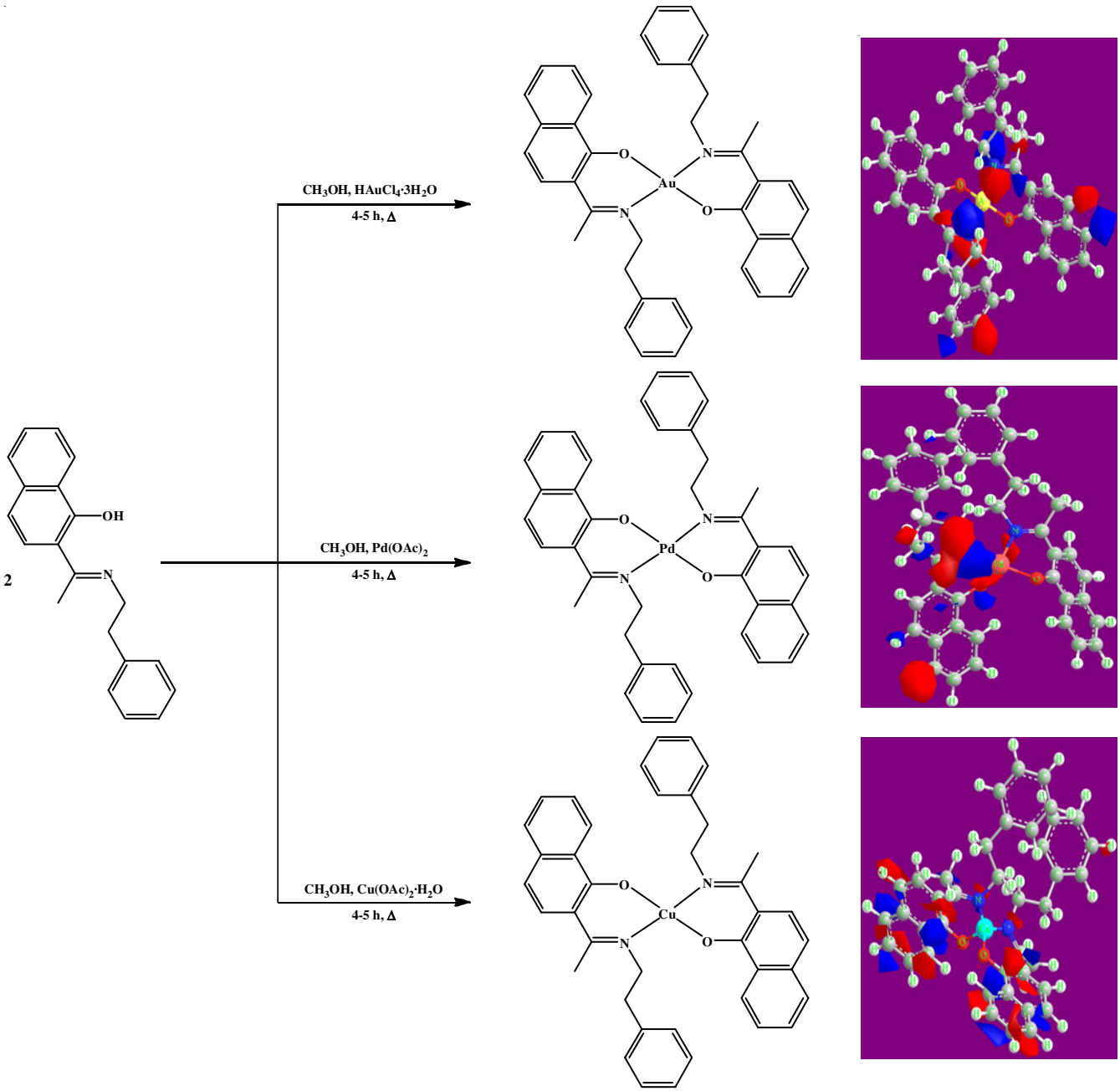

Scheme-II: Proposed synthesized metal complexes M(L)$_2$ and its optimized shape

(ppm): 2.289 (s, -CH_3, 3H), 3.151 (t, -CH_2, 2H), 3.849 (t, N-CH_2, 2H), 6.996-8.648 (m, Ar-H, 11H). ESI-MS (*m/z*): 773.24 (100.0%).

$Pd^{II}(L)_2$ complex [*bis*((2-((E)-1-(phenethylimino)ethyl)-naphthalen-1-yl)oxy)palladium]: m.f.: $C_{40}H_{36}N_2O_2Pd$, *m.w.*: 683.16, yield: 590.49 mg (73%), colour: brown, m.p.: 256-258 ºC. Elemental analysis calcd. (found) %: C, 70.24 (70.33); H, 5.21 (5.31); N, 4.06 (4.10); O, 4.61 (4.68); Pd, 15.51 (15.58). FT-IR (KBr, ν_{max}, cm^{-1}): 1577.72 (C=N), 1556.50-1452.88 (C=C), 1250.38 (C-O), 1022.10 (C-N-C). ^1H NMR (400, $CDCl_3$), δ (ppm): 2.294 (s, -CH_3, 3H), 3.501 (t, -CH_2, 2H), 4.343 (t, N-CH_2, 2H), 7.005-8.360 (m, Ar-H, 11H). ESI-MS (*m/z*): 682.18 (100.0%).

$Cu^{II}(L)_2$ complex [*bis*((2-((E)-1-(phenethylimino)ethyl)-naphthalen-1-yl)oxy)copper]: *m.f.*: $C_{40}H_{36}N_2O_2Cu$, *m.w.*: 640.29, yield: 560.72 mg (76%), colour: brown, m.p.: 244-246 ºC. Elemental analysis calcd. (found) %: C, 71.94 (72.03); H, 5.66 (5.76); N, 3.91 (4.00); O, 9.07 (9.14); Cu, 9.02 (9.92). FT-IR (KBr, ν_{max}, cm^{-1}): 1577.70 (C=N), 1550.70-1451.98 (C=C), 1250.42 (C-O), 1024.15 (C-N-C). ^1H NMR (400, $CDCl_3$), δ (ppm): 2.288 (s, -CH_3, 3H), 3.121 (t, -CH_2, 2H), 3.823 (t, N-CH_2, 2H), 6.637-8.869 (m, Ar-H, 11H). ESI-MS (*m/z*): 639.21 (100.0%).

RESULTS AND DISCUSSION

A novel Schiff base ligand was obtained as a result of the condensation of 1-hydroxy-2-acetonaphthone (HAN) and phenylethylamine (PEA). Stable coloured complexes were obtained when synthesized Schiff base ligand interacted with the Au(III), Pd(II) and Cu(II) ions. All the metal complexes are soluble in mostly organic polar solvents *e.g.* $CHCl_3$, CH_2Cl_2, DMSO, DMF and acetone. However, in *n*-hexane and dry petroleum ether, all the synthesized metal complexes are insoluble.

UV-vis spectra: The UV-visible absorption spectra of Schiff base ligand (HL) and its metal complexes were obtained in methanol solvent. The Schiff base exhibits five main peaks at 225.50, 271.00, 287.00, 322.50 and 409.00 nm. The band at 225-300 nm is due to the π→π* transition of aromatic rings of ligand, while the bands at 300-350 nm involve the π→π* transition of -C=N- chromophore of ligand (Fig. 1a). The longer wavelength peaks over 400 nm can be assigned to the intramolecular charge interactions of n→π* transition of non-bonding electrons present on the Schiff base compound [25]. Furthermore, the phenolic OH and imine C=N groups of the ligand were involved in the metal-ligand charge transfer (MLCT) transitions in the metal complexes by shifting the electronic absorption band toward lower energy, which means longer wavelength. Bands with longer wavelengths (< 409 nm) are ascribed to the d→d transitions in complexes [26] (Fig. 1b-c).

FT-IR spectra: Table-1 shows the key IR frequencies of the ligands and its corresponding metal complexes. The ligand exhibits a strong band centred at 3424.01 cm^{-1}, showing the existence of a phenolic-OH group with a wide including intra-intermolecular hydrogen bonding. The aromatic and aliphatic C-H groups are most likely responsible for the weak bands found in the 3080-2860 cm^{-1} region. However, the key IR bands of the metal complexes at 1577.70, 1577.72 and 1577.70 cm^{-1} (gold, palladium and copper complexes) were shifted from the upper wavenumber at 1591.53 cm^{-1} to the lower wavenumber by 13-14 cm^{-1}. When compared to neat azomethine group, the appearance of this shifting demonstrates that the free ligand is effectively coordinated to the metallic ions. Furthermore, high intensity bands were observed around 1271.38 cm^{-1} for phenolic C-O vibrations confined at spanning oxygen and appearing between 1256.50, 1250.38 and 1250.42 cm^{-1} for the studied metal complexes. The alteration in phenolic absorption frequency, showing coordination to metal ion *via* oxygen atom of phenolic -OH group.

NMR spectra: In ^1H NMR spectra of ligand HL, the proton of phenolic-OH was observed as a singlet at 16.414 ppm [27]. Aromatic proton signals for Schiff base ligand and its metal complexes resonant as multiplate in the 6.627-8.869 ppm range. At δ 3.820 and δ 3.107 ppm, two ethylene chain triplet signals, N=CH_2-CH_2-Ar, were observed in the ligand and these same triplet signals were also observed downfield in the metal chelates. Methyl protons of the ligand, with the formula -N=C-

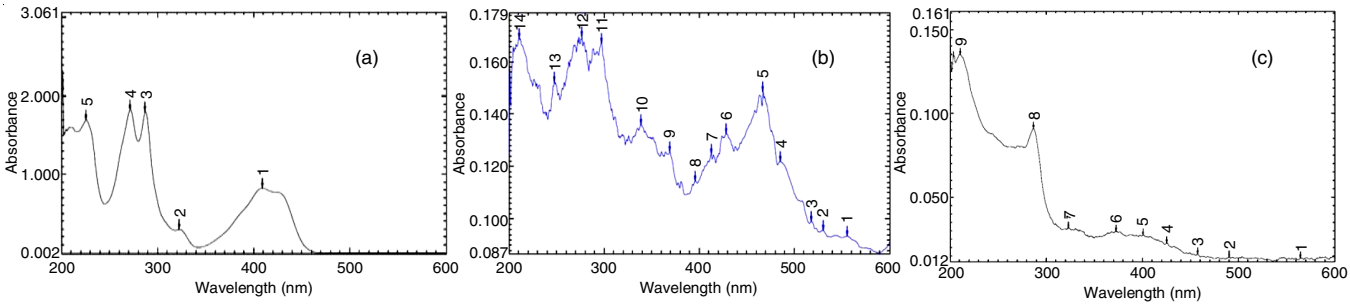

Fig. 1. UV-Vis spectra of Schiff base ligand (LH) (a), $Au(L)_2$ complex (b) and $Cu(L)_2$ complex (c)

TABLE-1
FT-IR SPECTRAL ANALYSIS OF SCHIFF BASE AND ITS METAL COMPLEXES

Compound	ν(-OH)	ν(H_2O)	ν(C=C–H)	ν(C=N–)	ν(C–O)	ν(C-N-C)
HL	3424.01	–	3059.89	1591.53	1271.38	1022.21
$Au(L)_2$	–	3429.81	3056.18	1577.70	1256.50	1021.58
$Pd(L)_2$	–	3419.39	3056.00	1577.72	1250.38	1022.10
$Cu(L)_2$	–	3425.29	3055.97	1577.70	1250.42	1024.15

CH_3, are responsible for the peak about δ 2.255 ppm and they are slightly affected by metal complexes. All of the protons' signals in the synthesized metal complexes have been moved toward the downfield in comparison to the ^{1}H NMR spectra of the ligand, which further confirmed that a metal ion has been complexed with the ligand.

^{13}C NMR spectra: In the ^{13}C NMR spectrum of ligand HL, a signal at δ 175.789 ppm was visible, which is due to the azomethine carbon. A signal appeared at δ 170.768 ppm was caused by an oxygen atom that contained aromatic carbon, while the peaks at δ 137.718-108.086 ppm confirmed the aromatic ring. The peaks of ethyl chain and methyl group were observed at 46.327 ppm, 35.402 ppm and 13.585 ppm for methylene (-N-CH_2-), (Ar-CH_2-) and methyl (-N=C-CH_3), respectively. Thus, the formation of the Schiff base ligand metal complex is confirmed by all these characteristics of the ^{13}C NMR spectrum.

LC-MS: A molecular ion peak at *m/z* 290.2 was visible for the Schiff base ligand HL which is comparable to its molecular weight (Fig. 2a). Similar molecular ion peaks were also visible in the ESI mass spectra of the corresponding metal complexes. The metal complexes of gold [Au($C_{40}H_{36}N_2O_2$)], palladium [Pd($C_{40}H_{36}N_2O_2$)] and copper [Cu($C_{40}H_{36}N_2O_2$)] corresponds to a molecular ion peak at *m/z* 773.71, *m/z* 683.16, *m/z* 640.29, respectively (Fig. 2b-c).

SC-XRD: Single crystals of ligand HL with proper size were employed to collect data at 273 K using a Bruker D8 Venture diffractometer (Table-2). The molecular structure was resolved using direct methods and refined using full-matrix least squares on F^2 with the SHELXL-2019/1 software. Using programme Olex2 1.5, multi-scan empirical absorption adjustments were applied to the data. The ORTEP diagram of ligand HL in Figs. 3 and 4 reveals that the H atoms are positioned in their optimal geometrical places and controlled to ride on their maternal atoms and the non-hydrogen atoms, which have sophisticated anisotropic thermal constraints. In single crystal structure of Schiff base HL, the azomethine group presents an E configuration between the PEA and HAN fragments, with a torsion angle N1-C11-C8-C9 of 175.09(18)º. Similarly, structure of HL displays a torsion angle N1-C13-C14-C15 of 179.96(18)º (Table-3), which is consistent with an anti-staggered conformation regarding rotation around C13–C14 bond [28]. Schiff base HL is connected by O–H···N hydrogen bonding interactions at a distance of 1.801 Å between the hydroxyl group and the imine nitrogen atom (Table-4). These hydrogen bonds lead to the formation of zigzag chains along the *c*-axis, which results in the formation of corrugated layers (Fig. 5).

PXRD studies: When compared to the reported spectra using the peak matching approach, the synthesized Schiff base ligand and its complex were allocated to fine X-ray peaks that supported the comparison and formation of metal complexes with Schiff base ligand. The XRD patterns of the synthesized

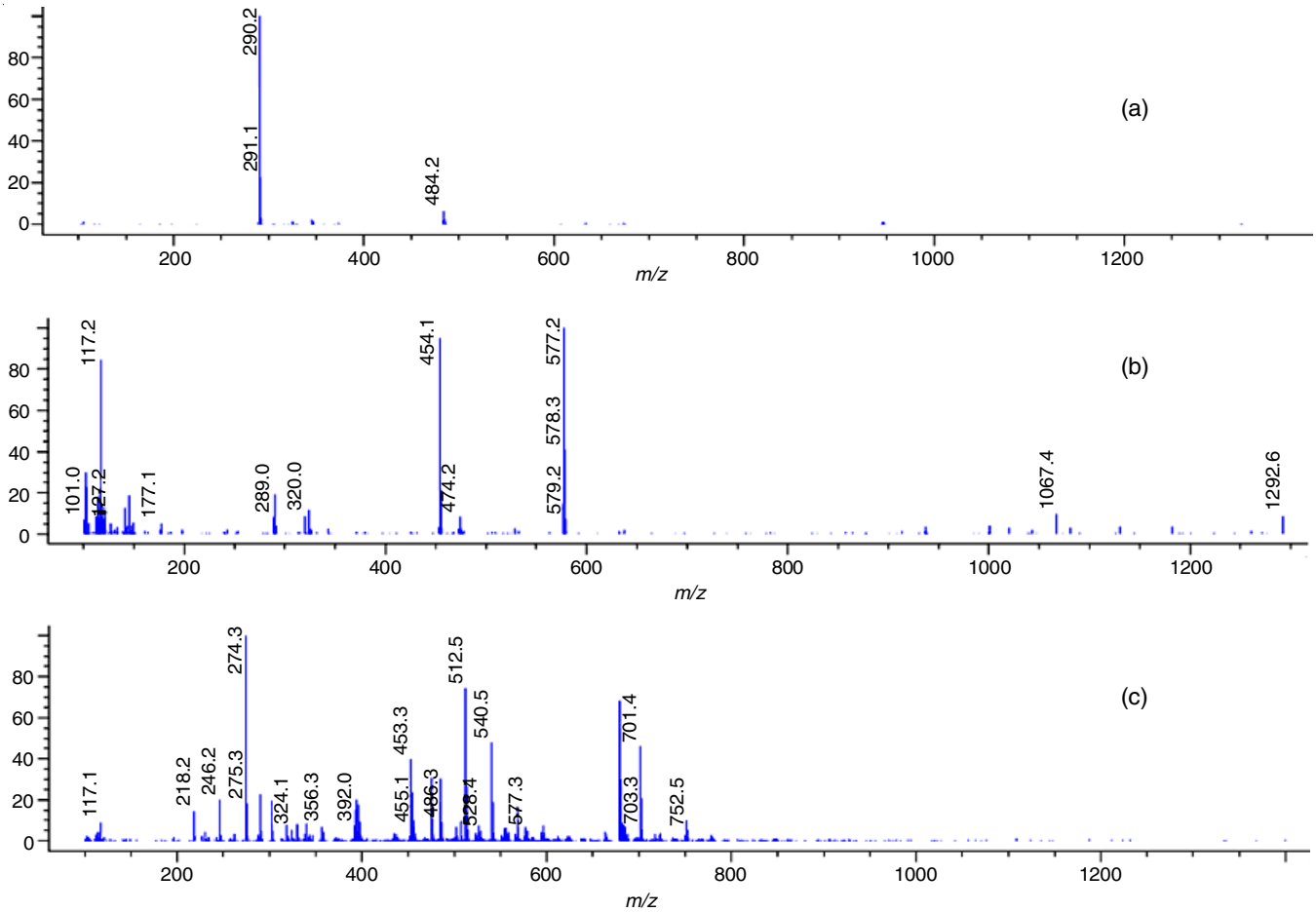

Fig. 2. Mass spectra of LH (a), $Au(L)_2$ (b) and $Pd(L)_2$ (c)

TABLE-2
CRYSTAL DATA AND STRUCTURE
REFINEMENT OF SCHIFF BASE LIGAND (HL)

Compound	HL
Empirical formula	$C_{20}H_{19}NO$
Formula weight	289.380
Temperature/K	273.15
Crystal system	Monoclinic
Space group	$P2_1/n$
a (Å)	7.3455(4)
b (Å)	16.8577(8)
c (Å)	12.7384(6)
α (°)	90
β (°)	93.329(2)
γ (°)	90
Volume (Å)^3	1574.71(14)
Z	4
ρ_{calc} (g/cm^3)	1.221
μ (mm^{-1})	0.075
F(000)	616.3
Crystal size (mm^3)	0.03 × 0.023 × 0.0214
Radiation	Mo Kα (λ = 0.71073)
2θ range for data collection (°)	4.02 to 54.24
Index ranges	$-9 \le h \le 9, -21 \le k \le 21, -16 \le l \le 16$
Reflections collected	48422
Independent reflections	3486 [R_{int} = 0.0543, R_{sigma} = 0.0245]
Data/restraints/parameters	3486/0/202
Goodness-of-fit on F^2	1.086
Final R indexes [I> = 2σ(I)]	R_1 = 0.0609, wR_2 = 0.1806
Final R indexes [all data]	R_1 = 0.0823, wR_2 = 0.2032
Largest diff. peak/hole/e Å^{-3}	0.50/-0.37

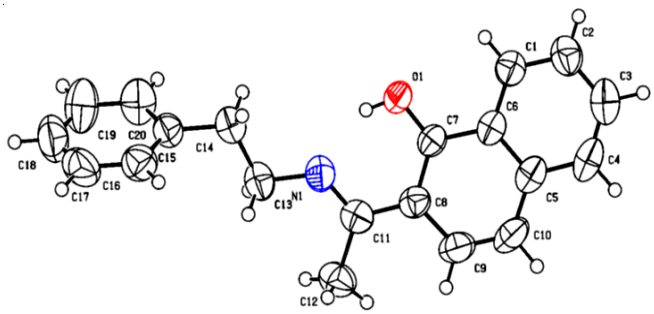

Fig. 3. ORTEP diagram of Schiff base ligand HL with 50% probability ellipsoids

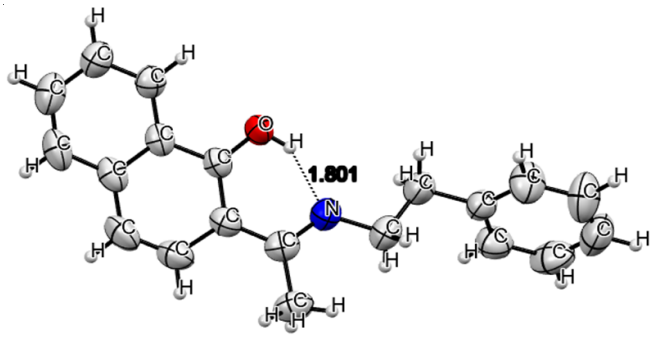

Fig. 4. ORTEP diagram of Schiff base ligand HL with intramolecular hydrogen bonding 50% probability ellipsoids

metal complexes revealed that all of the peaks, as well as few additional peaks caused due to the metal chelation, were present [29,30]. Schiff base ligand HL shows the peaks at

TABLE-3
BOND ANGLES OF SYNTHESIZED SCHIFF BASE (HL)

Atomic bond	Angle (°)	Atomic bond	Angle (°)
C11-N1-C13	125.69(17)	C6-C7-O1	118.75(16)
C17-C18-C19	120.0(2)	C6-C7-C8	118.26(15)
C20-C19-C18	120.3(3)	C1-C6-C7	120.40(16)
C15-C20-C19	121.6(3)	C5-C6-C7	120.72(17)
C14-C15-C20	120.3(2)	C5-C6-C1	118.88(17)
C16-C15-C20	118.5(2)	C2-C1-C6	120.82(19)
C16-C15-C14	121.2(2)	C3-C2-C1	120.2(2)
C13-C14-C15	112.47(17)	C4-C3-C2	120.7(2)
C14-C13-N1	110.26(16)	C16-C17-C18	119.8(2)
C8-C11-N1	118.90(17)	C17-C16-C15	119.8(2)
C12-C11-N1	119.05(19)	C5-C4-C3	120.9(2)
C12-C11-C8	122.05(18)	C4-C5-C6	118.5(2)
C7-C8-C11	120.26(16)	C10-C5-C6	118.61(18)
C9-C8-C11	121.67(18)	C10-C5-C4	122.93(19)
C9-C8-C7	118.07(18)	C9-C10-C5	121.48(18)
C8-C7-O1	122.98(16)	C10-C9-C8	122.73(19)

TABLE-4
BOND LENGTHS OF SYNTHESIZED SCHIFF BASE (HL)

Atomic bond	Length (Å)	Atomic bond	Length (Å)
O1-C7	1.273(2)	C8-C7	1.439(3)
N1-C13	1.466(2)	C8-C9	1.433(3)
N1-C11	1.308(2)	C7-C6	1.453(2)
C18-C19	1.351(4)	C6-C1	1.406(3)
C18-C17	1.380(5)	C6-C5	1.408(2)
C19-C20	1.359(4)	C1-C2	1.371(3)
C20-C15	1.381(3)	C2-C3	1.379(3)
C15-C14	1.506(3)	C3-C4	1.358(3)
C15-C16	1.372(3)	C17-C16	1.396(4)
C14-C13	1.501(3)	C4-C5	1.415(3)
C11-C8	1.425(3)	C5-C10	1.430(3)
C11-C12	1.500(3)	C10-C9	1.333(3)

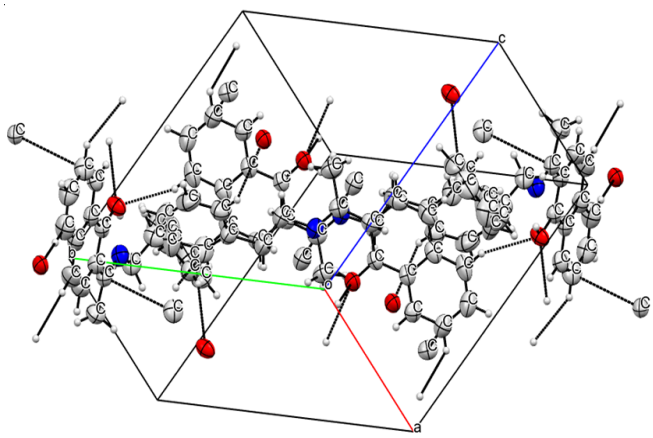

Fig. 5. Packing cell diagram of Schiff base Ligand HL with 50% probability ellipsoids

13.846°, 17.213°, 20.966°, 24.357°, 28.241°, 29.858° and 34.869°, which demonstrates that the synthesized Schiff base are polycrystalline in nature (Fig. 6). The highest intensity peak of $Au(L)_2$, $Pd(L)_2$ and $Cu(L)_2$ complexes were observed at 38.165°, 18.611° and 24.971°, respectively have lower intensity than the ligand (Fig. 7). The crystal system, space group, unit cell volume parameters of the synthesized Schiff base ligand and its corresponding metal complexes are given in Table-5.

TABLE-5
POWDER X-RAY DIFFRACTION DATA OF SCHIFF BASE AND ITS METAL COMPLEXES

Compound	$L(C_{20}H_{19}NO)$	$Au(C_{20}H_{18}NO)_2$	$Pd(C_{20}H_{18}NO)_2$	$Cu(C_{20}H_{18}NO)_2$
Empirical formula	$C_{20}H_{19}NO$	$C_{40}H_{36}AuN_2O_2$	$C_{40}H_{36}N_2O_2Pd$	$C_{40}H_{36}CuN_2O_2$
Formula weight	289.38	773.71	683.16	640.29
Temperature (K)	298	298	298	298
Crystal system	Tetragonal	Cubic	Monoclinic	Monoclinic
Lattice type	P	P	P	P
a (Å)	5.250244	4.078906	11.64704	22.835430
b (Å)	5.250244	4.078906	7.117175	4.640581
c (Å)	25.42294	4.078906	9.777458	8.144105
α (°)	90.00000	90.00000	90.000000	90.000000
β (°)	90.00000	90.00000	103.1942	107.221911
γ (°)	90.00000	90.00000	90.000000	90.000000
Unit cell volume (Å^3)	700.78494	67.86270	789.09750	824.33

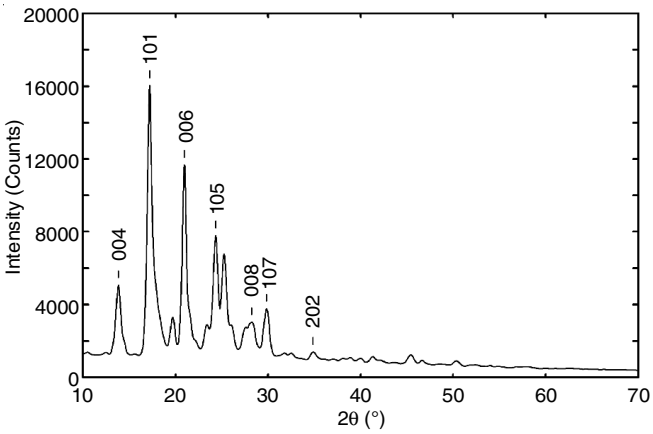

Fig. 6. XRD spectra of Schiff base ligand (HL)

TGA-DSC: TGA/DSC thermogram of Au(III) complex show three step decomposition, when heating the sample gradually, an endothermic peak was observed from the DSC analysis after the coordinated water molecules and ligands -CH_3 group were eliminated in the first stage commencing from 25 to 302.25 ºC. In the second step, at the temperature range of 302.25 to 348.67 ºC, approx. 32.44 % (0.4791 mg) weight was lost due to this an endothermic peak, which is attributed to the removal of non-coordinated part of ligand. Finally, in the third step, in the temperature range of 348.67 to 900 ºC gradually decrease the mass of complex and lastly gold oxide and carbon residue leftovers (Fig. 8). Furthermore in the Pd(II) complex, TGA/DSC thermogram can also be explained in three steps. Beginning from 25 to 257.01 ºC, the curve shows the elimination of

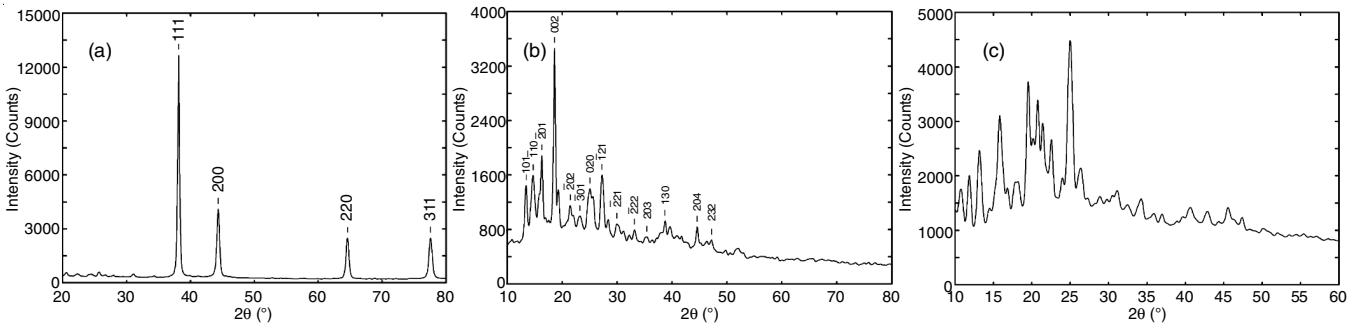

Fig. 7. XRD spectra of $Au(L)_2$ complex (a), $Pd(L)_2$ complex (b) and $Cu(L)_2$ complex (c)

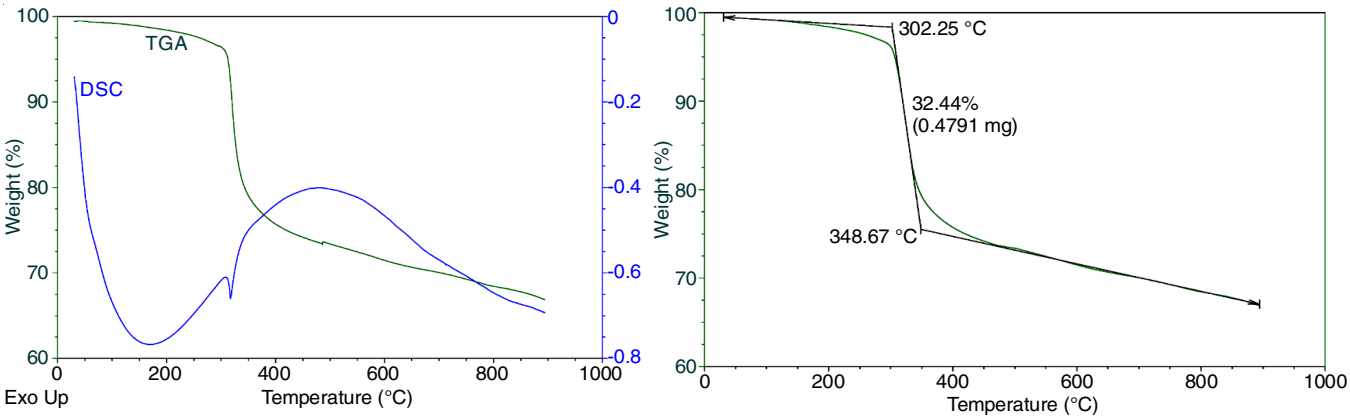

Fig. 8. Thermal analysis of $Au(L)_2$ complex: DSC (a) and TA (b) thermograms

lattice water molecules and CH_3 group of ligand. This stage in the DSC graph shows the endothermic reactions. In second step, the majority of the complex losses occur in the temperature range of 257.01-300.49 ºC, resulting in a weight loss of 92.55% (1.328 mg). Additionally, it comprises of an endothermic step in the DSC peaks. In third step, at the temperature range between 300.49 and 900 ºC, the palladium metal complex is converted into palladium oxide and the carbon residue is left behind (Fig. 9). Similarly in Cu(II) complex, TGA/DSC curves explains the three steps, first of all starting temperature at 25 to 263.81 ºC indicates the elimination of lattice water molecules and ligands -CH_3 group. The second stage involves an endothermic step in the DSC peaks due to the non-coordinated Schiff base ligand, and involves the loss of 78.79% of the complex from 263.81 to 306.57 ºC (1.080 mg). In the third step, a broad exothermic peak observed in the same region in DSC, which corresponds to rapidly degradation of corresponding part of ligand occured between 306.57 and 900 ºC and results in a weight loss of copper metal complex and left copper oxide and carbon residue (Fig. 10).

***In vitro* Antibacterial activity:** *In vitro* antibacterial activity of the synthesized Schiff base ligand and its corresponding metal complexes was done by screening them against two Gram-negative *Escherichia coli*, *Pseudomonas aeruginosa* and Gram-positive *Staphylococcus aureus*, *Bacillus subtilis* bacteria. Both Gram-positive and Gram-negative bacterial strains are susceptible to the effects of synthesized compounds. According to the Tweedy's chelation theory and Overtone's concept, metal complexes have greater antibacterial activity than the free ligand [31]. All the synthesized metal complexes exposed greater activity at the concentration of 1000 µg than at other values as shown in Table-6.

***In vitro* antifungal activity:** In contrast to the fungal species *Candida albicans* and *Aspergillus niger* which were cultivated on potato dextrose agar medium, the antifungal activity of Schiff base ligand and complexes was investigated *in vitro* and the results of the antifungal activity using the disc diffusion method are shown in Table-6. Schiff base ligand and its metal complexes exhibited higher activity than ciprofloxacin reference drug. Additionally, HL ligand's antifungal bioactivity increases when it is coordinated with the studied metal ions. Among these metal complexes, moderate antifungal activity was reported in Au(III) and Pd(II) metal complexes.

Antioxidant activity: The antioxidant activity of the Schiff base ligand and metal complexes were assessed using the DPPH technique and compared to standard ascorbic acid. The outcomes of the free radical scavenging activity of synthesized compounds at different concentrations are shown in Table-7. The activity of the synthesized metal complexes are higher than that of the free Schiff base. Increased antioxidant activity is a result of the metal ions' ability to remove electrons, which makes it easier for hydrogen to be released and diminish DPPH radicals. The Pd(II) complexes among them shown better scavenging activity than Au(III) and Cu(II) complexes.

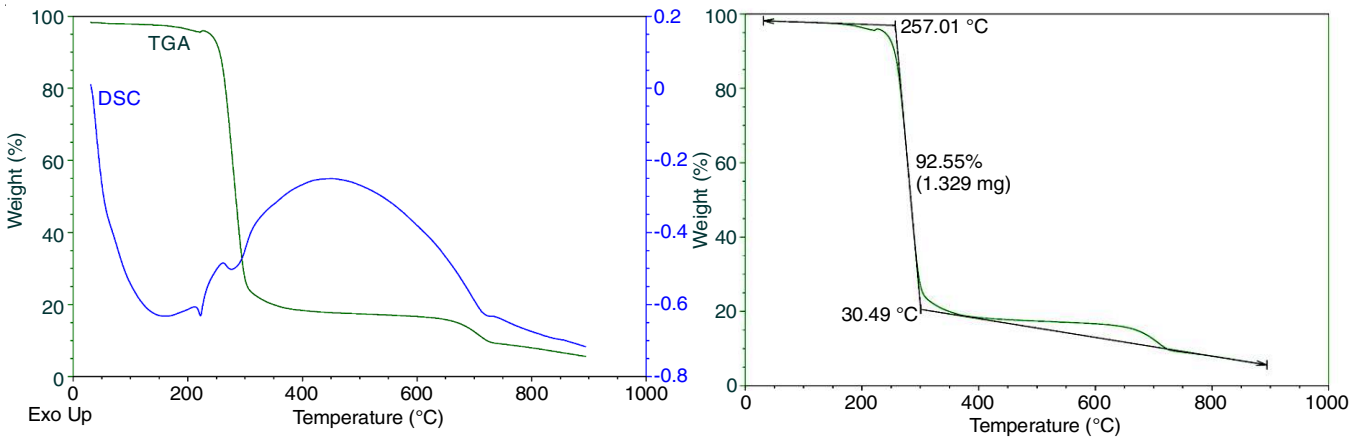

Fig. 9. Thermal analysis of $Pd(L)_2$ complex: DSC (a) and TA (b) thermograms

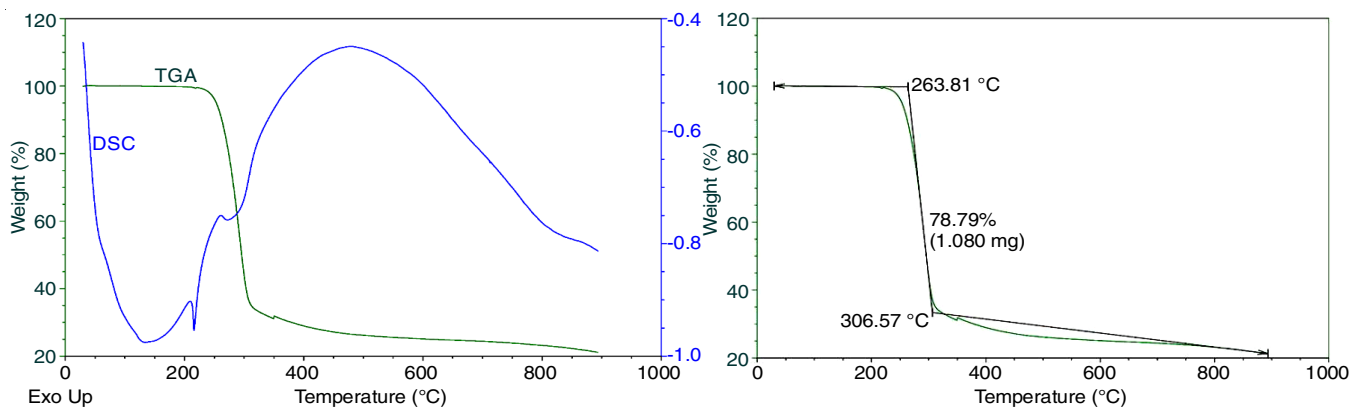

Fig. 10. Thermal analysis of $Cu(L)_2$ complex: DSC (a) and TA (b) thermograms

TABLE-6
ANTIMICROBIAL ACTIVITY DATA OF SCHIFF BASE AND ITS METAL COMPLEXES (mm)

Compound	Conc. (µg/mL)	Antibacterial activity				Antifungal activity	
		E. coli	*P. aeruginosa*	*S. aureus*	*B. subtilis*	*C. albicans*	*A. niger*
HL	1000	9	10	12	8	6	8
	500	9	8	9	8	6	6
	250	6	7	7	7	5	6
	125	6	7	6	–	–	5
	50	–	6	–	–	–	–
$Au(L)_2$	1000	16	15	17	16	11	10
	500	10	12	11	9	8	9
	250	9	10	10	8	7	7
	125	6	7	7	6	6	6
	50	–	6	–	–	–	–
$Pd(L)_2$	1000	18	17	17	16	13	11
	500	12	12	13	14	11	10
	250	8	9	9	12	7	7
	125	6	7	7	8	6	–
	50	6	–	7	7	–	–
$Cu(L)_2$	1000	15	13	14	15	12	10
	500	10	11	9	9	8	7
	250	7	8	7	7	8	7
	125	7	8	7	6	6	–
	50	6	7	6	6	–	–
Ciprofloxacin std. drug	20	39	31	33	28	5	5

TABLE-7
ANTIOXIDANT ACTIVITY OF SYNTHESIZED SCHIFF BASE AND ITS METAL COMPLEXES

Conc. (µg/mL)	Ascorbic acid*	HL	$Au(L)_2$	$Pd(L)_2$	$Cu(L)_2$
10	16.9507	3.5129	3.9029	1.6708	0.6241
50	16.4126	6.4393	2.4501	2.651	1.8463
100	32.6457	9.7891	6.7271	6.228	1.9602
250	61.1659	13.7319	7.2574	16.3765	3.9846
500	75.6951	13.3571	15.7612	28.1191	6.0297
1000	88.1614	14.42117	31.8909	62.6905	8.4588
2500	88.7892	9.0245	38.5411	99.667	8.3928

*Standard reference drug

Conclusion

Metal complexes of Au(III), Pd(II) and Cu(II) were synthesized with unsymmetrical bidentate Schiff base ligand 2-(1-(phenethylimino)ethyl)naphthalen-1-ol. Various spectral techniques such as UV-visible, FT-IR, ^{1}H NMR, ^{13}C NMR, LCMS, SC-XRD, PXRD and TGA-DSC were utilized to characterize them. The coordination of naphthol-oxygen and azomethine-nitrogen atoms in the physico-chemical results show that Au(III), Pd(II) complexes have a square-planar geometry while Cu(II) complexes have a distorted square planar. All the synthesized three metal complexes were found to exhibit stronger antibacterial and antifungal activities than those of their parent ligand. In comparison to the standard ascorbic acid at a concentration of 2500 µg/mL, the antioxidant activity of Pd(II) metal complex is outstanding. All of these results led to the conclusion that the bidentate NO Schiff base and their metal complexes are a rich source of information on coordination molecules and have the potential to be useful biological agents.

Supplementary materials: CCDC 2193423 contain the supplementary crystallographic data for Schiff base ligand. These data can be obtained free of charge *via* http://www.ccdc.cam.ac.uk/conts/retrieving.html or from the Cambridge Crystallographic Data Centre, 12 Union Road, Cambridge CB2 1EZ, UK; fax: (+44) 1223-336-033 or e-mail: deposit@ccdc.cam.ac.uk

ACKNOWLEDGEMENTS

The authors are thankful to IIT Hyderabad for SC-XRD, TGA-DSC spectral analysis, University of Hyderabad and Simson Life Science, Hyderabad, India for LCMS, ^{1}H NMR, ^{13}C NMR, FT-IR, UV-VIS spectral facilities.

CONFLICT OF INTEREST

The authors declare that there is no conflict of interests regarding the publication of this article.

REFERENCES

1. A. Atahan and S. Durmus, *Spectrochim. Acta A Mol. Biomol.*, **144**, 61 (2015); https://doi.org/10.1016/j.saa.2015.01.085
2. S. Bag, P.K. Bhaumik, S. Jana, M. Das, P. Bhowmik and S. Chattopadhyay, *Polyhedron*, **65**, 229 (2013); https://doi.org/10.1016/j.poly.2013.08.028
3. B.T. Vhanale, N.J. Deshmukh and A.T. Shinde, *Heliyon*, **5**, e02774 (2019); https://doi.org/10.1016/j.heliyon.2019.e02774
4. F.T. Esmadi, O.F. Khabour, K. Abbas, A.E. Mohammad, R.T. Obeidat and D. Mfady, *Drug Chem Toxicol.*, **39**, 41 (2016); https://doi.org/10.3109/01480545.2015.1017882
5. S. Kumar, D.N. Dhar and P.N. Saxena, *J. Sci. Ind. Res.*, **68**, 181 (2009); http://nopr.niscpr.res.in/handle/123456789/3170
6. Y.M. Ahmed, M.M. Omar and G.G. Mohamed, *J. Iran. Chem. Soc.*, **19**, 901 (2022); https://doi.org/10.1007/s13738-021-02359-w
7. M. Pal, D. Musib and M. Roy, *New J. Chem.*, **45**, 1924 (2021); https://doi.org/10.1039/D0NJ04578K

9. S. Makar, T. Saha and S.K. Singh, *Eur. J. Med. Chem*., **161**, 252 (2019); https://doi.org/10.1016/j.ejmech.2018.10.018
9. M.A. Abozeid, A.A. El-Sawi, M. Abdelmoteleb, H. Awad, M.M. Abdel-Aziz, A.-R.H. Abdel-Rahmana and E.-S.I. El-Desoky, *RSC Adv*., **10**, 42998 (2020); https://doi.org/10.1039/D0RA08526J
10. P. Pandey, A. Verma, K. Bretosh, J. Sutter and S.S. Sunkari, *Polyhedron*, **164**, 80 (2019); https://doi.org/10.1016/j.poly.2019.02.037
11. A.S. Al-Bogami, A.M. Al-Majid, M.A. Al-Saad, A.A. Mousa, S.A. Al-Mazroa and H.Z. Alkhathlan, *Molecules*, **14**, 2147 (2009); https://doi.org/10.3390/molecules14062147
12. C. Balakrishna, V. Kandula, R. Gudipati, S. Yennam, P.U. Devi and M. Behera, *Synlett*, **29**, 1087 (2018); https://doi.org/10.1055/s-0036-1591898
13. D. Banik, J. Kuchlyan, A. Roy, N. Kundu and N. Sarkar, *J. Phys. Chem. B*, **119**, 2310 (2015); https://doi.org/10.1021/jp5064879
14. S. Roy, A. Maity, N. Mudi, M. Shyamal and A. Misra, *Photochem. Photobiol. Sci*., **18**, 1342 (2019); https://doi.org/10.1039/c8pp00558c
15. N. Sarkar, P.K. Bhaumik, S. Chattopadhyay, *Polyhedron*, **115**, 37 (2016); https://doi.org/10.1016/j.poly.2016.04.013
16. B.T. Vhanale and A.T. Shinde, *J. Iran. Chem. Soc.*, **19**, 2641 (2022); https://doi.org/10.1007/s13738-021-02486-4
17. B. Vhanale, D. Kadam and A. Shinde, *Heliyon*, **8**, e09650 (2022); https://doi.org/10.1016/j.heliyon.2022.e09650
18. J.M. Lee, S.Y. Shin, H. Yoon, M.S. Lee, Y.R. Lee, D. Koh and Y.H. Le, *J. Korean Soc. Appl. Biol. Chem*., **56**, 343 (2013); https://doi.org/10.1007/s13765-013-3065-1
19. D. Ashok, K. Padmavati, B.V. Lakshmi and M. Sarasija, *Chem Heterocycl Compd*., **52**, 15 (2016); https://doi.org/10.1007/s10593-016-1824-8
20. S.R.M. Ibrahim and G.A. Mohamed, *Phytochem Rev*., **15**, 279 (2016); https://doi.org/10.1007/s11101-015-9413-5
21. C.M. da Silva, D.L. da Silva, L.V. Modolo, R.B. Alves, M.A. de Resende, C.V.B. Martins and A. de Fa´tima, *J. Adv. Res*., **2**, 1 (2011); https://doi.org/10.1016/j.jare.2010.05.004
22. M.S. More, P.G. Joshi, Y.K. Mishra and P.K. Khanna, *Mater. Today Chem*., **14**, 100195 (2019); https://doi.org/10.1016/j.mtchem.2019.100195
23. D.M. Boghaei and M. Lashanizadegan, *Synth. Reacx. Inorg. Met.-Org. Chem*., **30**, 1393 (2000); https://doi.org/10.1080/00945710009351841
24. D. Aggoun, M. Fernández-García, B. Bouzerafa, Y. Ouennoughi, D. López, F. Setifi and A. Ourari, *Polyhedron*, **187**, 114640 (2020); https://doi.org/10.1016/j.poly.2020.114640
25. A.A. Ardakani, H. Kargar, N. Feizi and M.N. Tahir, *J. Iran. Chem. Soc*., **15**, 1495 (2018); https://doi.org/10.1007/s13738-018-1347-6
26. S.R. Salman and F.S. Kamounah, *Spectroxc Lett*., **35**, 327 (2002); https://doi.org/10.1081/SL-120005669
27. A. Kumar, M. Agarwal and A.K. Singh, *J. Organomet. Chem*., **693**, 3533 (2008); https://doi:10.1016/j.jorganchem.2008.07.024
28. S. Chaves, A. Pérez-Redondo and R. Quevedo, *J. Chem. Crystallogr*., **50**, 206 (2020); https://doi.org/10.1007/s10870-019-00792-7
29. A. Palanimurugan and A. Kulandaisamy, *Asian J. Chem*., **30**, 1262 (2018); https://doi.org/10.14233/ajchem.2018.21212
30. K.S.A. Abou Melhaa, G.A.A. Al-Hazmib and M.S. Refat, *Russ. J. Gen. Chem.*, **87**, 3043 (2017); https://doi.org/10.1134/S1070363217120519
31. P.K. Panchal, H.M. Parekh, P.B. Pansuriya and M.N. Patel, *J. Enzyme Inhib. Med. Chem*., **21**, 203 (2006); https://doi.org/10.1080/14756360500535229